

# Study of meiobenthos community in Manado Beach, North Sulawesi

*by Silvester Pratasik 26*

---

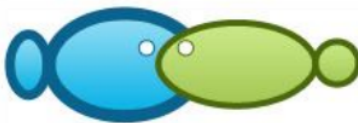
**Submission date:** 18-May-2021 09:32AM (UTC+0700)

**Submission ID:** 1588458797

**File name:** 2021.884-896-windarto.pdf (846K)

**Word count:** 6307

**Character count:** 30505



## Study of meiobenthos community in Manado Beach, North Sulawesi

Agung B. Windarto, Royke M. Rampengan, Esry T. Opa,  
Silvester B. Pratasik

2

Faculty of Fisheries and Marine Science, Sam Ratulangi University, Manado-95115, Indonesia. Corresponding author: S. B. Pratasik, spjong07@yahoo.com

**Abstract.** No study has documented the taxa composition of meiobenthos in North Sulawesi. This study was accomplished in Malayang Beach (station 1) and Tongkeina Beach (station 2). It aims to identify taxa and analyze the density, diversity, dominance, evenness, and the morphometry of meiobenthos, and to plot the granulometric distribution of the sediment. Samples were collected using purposive random sampling 7 cm long- spuit syringe of 1.5 cm diameter by inserting it as deep as 5 cm into the sediment (volume 8.84 cm<sup>3</sup>) and observed under a Stereo Microscope Brand Olympus Type CX 41. Results showed that there were 13 taxa found in station 1 and 15 taxa in station 2. The highest density of meiobent<sup>37</sup> in station 1 and station 2 were found in Harpacticoida and the lowest in Cyclopoida. The diversity in station 2 was high<sup>44</sup> than that in station 1, dominance in station 1 was higher than that in station 2, and the evenness in station 1 was lower than that in station 2. The meiobenthos morphometry of the cumulative eigen value of station 1 shows that the variance on axes 1 (F1) to 2 (F2) reaches 0.7066, meaning that the 70.66% of data variance could be explained up to the second axis, whereas the remaining 29.34% is explained by other axes (F2-F8). In station 2, the variance on axis 1 (F1) to axis 2 (F2) reaches 0.6761, meaning that 67.61% of data could be explained up to the second axis, and the remaining 32.29% is explained by other axes (F3-F8). If axis 3 (F3) is included to explain the variance of the data, the value reaches 80.85%. If the cumulative variance of the eigen value in both stations to the third axis (F3) does not reach 80%, then PCA could not be relied on to analyze the above problems. The sediment composition consisted of gravel 8.4%, coarse sands 9.86%, medium sand 8.84%, fine sand 51.24%, very fine sand 17.16% and dust 4.5%.

**Key Words:** taxa identification, density, diversity, dominance, evenness, sediment.

**Introduction.** Meiobenthos or meiofauna are benthic invertebrate organisms that live between sand grains or between sediments along the coast, especially in tidal area. Meiobenthos is defined based on the standard sieve with mesh size of 500 µm (1 000 µm) as the upper limit and 44 µm (63 µm) as the lower limit (Giere 2009). Stratified sieve meshes commonly used to filter meiofauna are 1.000 mm, 0.500 mm, 0.250 mm, 0.125 mm, 0.063 mm, and 0.044 mm. Meanwhile, Somerfield & Warwick (2013) also explained that meiofauna organisms are mobile metazoans that are smaller than macrofauna and larger than microfauna. According to Higgins & Thiel (1988), meiofauna is a group of benthic metazoans of 63-1,000 <sup>33</sup> or multicellular animals that live in spaces between sediment particles that can pass through a 500 µm filter and are retained in a 63 µm filter. Giere (2009) also explains that besides having permanent nature of life, there are also temporary meiofauna members. This group lives as meiofauna in larval phase, then settles and grows to macrofauna.

The main functions or roles of meiobenthos in the sea, according to Coull (1988), are to help enrichment or mineralization of organic matter in sediments, as a food source for benthos and larger demersal fish, so that the abundance of meiofauna makes the basic habitat of the waters be fertile or increases fertility, and to determine the water conditions in relation with contamination of organic matter, so that meiofauna can become a bioindicator of organic matter pollution in the waters.

There is no expert in the field of meiobenthology in Indonesia. Therefore, it is very important to provide scientific information as a basic reference in determining the conditions of a waterway in the Manado Beach area, North Sulawesi. The main limitation

1

AACL Bioflux, 2021, Volume 14, Issue 2.  
<http://www.bioflux.com.ro/aacl>

and difficulty in studying meiobenthos is at the taxonomic stage for species identification. The number of taxa in meiobenthos is also an obstacle that needs to be faced and developed (Giere 2009). This study aims to identify and analyze the composition of meiobenthos in Manado Beach, estimate the abundance and the density, analyze the community structure, measure and analyze the morphometric characteristics using ImageJ software, and analyze the sediment granulometry.

**Material and Method.** This work was carried out in July-August 2020 in Manado Beach, Manado City, North Sulawesi Province. Two locations were selected, station 1 (Malalayang Beach) and station 2 (Tongkaina Beach) (Figure 1). Sampling was done in intertidal zone using 3 parallel transect lines along 100 m coast as many as 5 random sampling points. It was accomplished using a corer of 7 cm, long syringe of 1.5 cm diameter inserted as far as 5 cm deep into the sediment (volume 8.84 cm<sup>3</sup>) following Coull & Chandler (2001), Giere (2009), Somerfield & Warwick (2013), and Eleftheriou (2013) and on the dry land of the two determined localities. The research station was determined based on the purposive sampling method under certain considerations. Malalayang Beach was chosen on the basis of the influence of local population activities and Tongkaina Beach was selected on the basis of tourist population activities. The meiofauna sampling point was determined using a random method (random sampling).

Sediment samples containing meiofauna were given 73.2 g MgCl<sub>2</sub> L<sup>-1</sup> – containing filtered seawater for anesthesia (anesthetics) and decantation. Lee (2018) stated that decantation is washing of samples-containing sand in 1 L-cylinder container (no more than 150 mL of sediment at one time) to separate meiofauna and sand by placing the sediment into a cylinder container and added with 1 L of freshwater. Then, it is shaken by reversing the cylinder 5-10 times to evenly distribute the sediment throughout the volume, and left for no more than 5 seconds until most of the solid particles (especially sand) fell down to the container bottom. The supernatant was carefully filtered through 1.0, 0.5, 0.063, and 0.044 µm sieves. This step was repeated 3-6 times. Rose Bengal mixed with 4% (1 g L<sup>-1</sup>) formaldehyde solution was given for preservation (fixation) as well as meiobenthos staining to make the meiobenthos be easily observed under a microscope, then the samples were brought to the laboratory to be extracted through decantation. Observations were done using a CX41-typed Olympus microscope. Meiobenthos identification followed Higgins & Thiel (1988), Giere (2009), and Eleftheriou (2013).



Figure 1. Study sites map (red dots).

**Potential analysis.** Meiobenthos sample collection followed Giere (2009) and Eleftheriou (2013) using corer of 1.5 cm diameter and 7 cm long syringe by inserting it 5 cm into the sediment (volume 8.84 cm<sup>3</sup>). Sampling used direct observation method through random survey in each station. Three sampling points were randomly selected for transects facilitated with 1 m<sup>2</sup> quadrat. The potential data were obtained in number and types of meiobenthos (calculated based on the individual meiobenthos taxon), and the identification was based on Higgins & Thiel (1988) and Giere (2009) manuals.

### **Ecological index analysis**

**Density.** Meiofauna was grouped into taxa and the density was calculated using Odum (1971) as follows:

$$Dm = \frac{n_i}{A} \times 10.000 \quad [24]$$

Where Dm = density index, n<sub>i</sub> is number of individual species or species i, A = cross-sectional area of the core multiplied by the number of replications (cm<sup>2</sup>), 10,000 is conversion value from cm<sup>2</sup> to m<sup>2</sup> (volume = 35.36; Deuteronomy = 10, A = 353.6 m<sup>2</sup>), and i = 1,2,3, ..., s.

**Diversity.** Diversity analysis used Shannon-Wiener's diversity index (Legendre & Legendre 2012) and Krebs (1989) as follows:

$$H' = -\sum_{i=1}^S P_i \ln P_i \quad [24]$$

where: H' is Shannon-Wiener diversity index, N = total number of individuals in the community (N =  $\sum n_i$ ), n<sub>i</sub> = number of species individuals or species i, P<sub>i</sub> = proportion of species i ( $n_i/N$ ), i = 1,2,3, ..., n, s is number of genera.

Based on the formula above, the Shannon-Wiener diversity index is categorized following Brower & Zar (1977) as shown below:

H' < 2.3026 = low population diversity;

2.3026 < H' < 6.9078 = moderate population diversity;

H' > 6.9078 = high population diversity.

**Dominance.** To calculate the dominance of meiobenthos, Simpson's dominance index (Krebs 1989) was used with the following equation:

$$D = \frac{1}{\sum_{i=1}^S (P_i)^2} \quad [24]$$

where: D is Dominance index, P<sub>i</sub> = proportion of species (taxa)i or ( $n_i/N$ ), i = 1,2,3, ..., n; N =  $\sum n_i$ , s = number of taxa.

The value of D ranges from 0 to 1 (Odum 1971) in which the value of D close to 0 indicates no individual dominance, and if the value of D approaches to 1 indicates that one genus or species dominates.

**Evenness.** Evenness which is manifested in the regularity index (equitability or evenness index) is a description of the distribution of the individuals of each species in the community. It was estimated following Krebs (1989):

$$E = \frac{H'}{H'_{\max}} \quad [30]$$

Then,

$$H'_{\max} = \ln S \quad [30]$$

where: E = evenness index;

H' = diversity index;

S = number of genera.

Evenness index ranges from between 0 and 1 (Odum 1971). The smaller the E value, the smaller the uniformity of a population, meaning that the distribution of the number of individuals of each species dominates the population. The greater the E value, the population shows uniformity, so that the number of individuals of each species can be said to be the same or not much different. Krebs (1989) states the value of the uniformity of a community as in Table 1.

Table 1  
Classification degree of evenness

<i>Evenness (E)</i>	<i>Criteria (the evenness index value range from 0 to 1)</i>
$0.00 < E \leq 0.50$	Community depressed condition or Low evenness stressed community
$0.50 < E \leq 0.75$	Moderate evenness, unstable community
$0.75 < E \leq 1.00$	Community stable condition

Source: Krebs (1989).

**Meiobenthos morphometric analysis.** ImageJ software was used to obtain meiobenthos morphometry. The variables measured by the ImageJ software programmatically are as follows:

- AA = The selected value is in square pixels. Area is a unit that is calibrated, such as square millimeter, square centimeter and others.
- PE = Perimeter is the length of the selection's outer boundary.
- CI = Circ. (circle):  $4\pi * \text{area} / \text{perimeter}^2$ . A value of 1.0 indicates a perfect circle. Getting closer to 0.0, this indicates an elongated shape. Value may not be valid for very small particles.
- F = Feret size is based on the statistic after rotating the object through all possible different angles. Feret Diameter is the longest distance between two points along the selected area, also known as the maximum caliper. Feret X and Feret Y are the coordinates of the initial Feret diameter (on X and Y axes).
- FX = Feret X is the coordinate of the initial Feret diameter (on X axis).
- FY = Feret Y is the coordinate of the initial Feret diameter (on Y axis).
- FA = Feret angle is the Feret value (0-180 degrees), the angle between the Feret diameter and the line parallel to the X axis of the image.
- MF = Feret is the minimum caliper diameter.
- AR = AR (aspect ratio): major\_axis / minor\_axes.
- RO = Rotation (roundness):  $4 * \text{area} / (\pi * \text{major\_axis}^2)$ , or the reciprocal of the aspect ratio.
- SO = Solidity: area / convex area.

**Sediment granulometry analysis.** The sediment granulometry was analyzed using sieving procedure to obtain a grain size classification in Wentworth scale and AFNOR scale. Furthermore, the granulometric distribution of the sediment was analyzed graphically to determine empirical mean, sorting, slope, and tapering. These four variables were calculated with the values shown by the sediment granulometric distribution graph based on the Folk and Ward model (Dyer 1986), followed with the interpretative criteria of the sorting, sloping, and tapering distribution value variables as follows:

a. Empirical mean (Mz):

$$Mz = (\varphi_{16} + \varphi_{50} + \varphi_{84}) / 3$$

b. Sorting ( $\sigma_1$ ):

$$\sigma_1 = (\varphi_{84} - \varphi_{16}) / 4 + (\varphi_{95} + \varphi_{5}) / 6,6$$

Criteria: <sup>28</sup>

$0.00 < \varphi_1 \leq 0.35 \Rightarrow$  very well sorted;  
 $0.35 < \varphi_1 \leq 0.50 \Rightarrow$  well sorted;

$0.50 < \varphi_1 \leq 1.00 \Rightarrow$  medium sorted;  
 $1.00 < \varphi_1 \leq 2.00 \Rightarrow$  badly sorted;  
 $2.00 < \varphi_1 \leq 4.00 \Rightarrow$  very badly sorted;  
 $\varphi_1 > 4.00 \Rightarrow$  very very badly sorted.

c. Skewness of the curve (Sk):

$$Sk = \left\{ (\varphi_{16} + \varphi_{84} - 2\varphi_{50}) / 2(\varphi_{84} - \varphi_{16}) \right\} + \left\{ (\varphi_{5} + \varphi_{95} - 2\varphi_{50}) / 2(\varphi_{95} - \varphi_{5}) \right\}$$

Criteria:

$-1.00 < Sk \leq -0.30 \Rightarrow$  asymmetric to firm size (very negative);  
 $-0.30 < Sk \leq -0.10 \Rightarrow$  asymmetric to large size (negative);  
 $-0.10 < Sk \leq +0.10 \Rightarrow$  symmetric granulometry;  
 $+0.10 < Sk \leq +0.30 \Rightarrow$  asymmetric to small size (positive);  
 $+0.30 < Sk \leq +1.00 \Rightarrow$  strong asymmetry to small size (very positive).

d. Curve kurtosis (Kg):

$$Kg = (\varphi_{95} - \varphi_{5}) / 2.44(\varphi_{75} - \varphi_{25})$$

Criteria:

$Kg \leq 0.67 \Rightarrow$  very platikurtic;  
 $0.67 < Kg \leq 0.90 \Rightarrow$  platikurtic;  
 $0.90 < Kg \leq 1.11 \Rightarrow$  mesokurtic;  
 $1.11 < Kg \leq 1.50 \Rightarrow$  leptokurtic;  
 $1.50 < Kg \leq 3.00 \Rightarrow$  very leptokurtic;  
 $Kg \leq 3.00 \Rightarrow$  the most leptokurtic.

**Principal component analysis.** The relationship between meiofauna measurement variables in Manado coastal waters used principal component analysis (PCA). Data analysis used Excel 2007 and version 14-adin ExcelStat software.

**Results.** The composition of the meiobenthos species found in Manado Beach consisted of 13 taxa in station 1 (Malalayang Beach), Ciliophora, Cladocera, Copepoda, Cyclopoida, Foraminifera, Harpacticoida, Kinorhyncha, Mollusca, Mite, Nematoda, Oligochaeta, Ostracoda and Tardigrada; and 15 taxa in station 2 (Tongkeina Beach), Ciliophora, Cladocera, Copepoda, Cyclopoida, Foraminifera, Harpacticoida, Kinorhyncha, Mollusca, Mite, Nematode, Oligochaeta, Ostracoda, Tardigrada and added two more taxa Polychaeta and Turbellaria (Table 2).

Table 2  
Composition of meiobenthos found in Manado Beach

No	Taxa	
	Station 1	Station 2
1	Ciliophora	Ciliophora
2	Cladocera	Cladocera
3	Copepoda	Copepoda
4	Cyclopida	Cyclopida
5	Foraminifera	Foraminifera
6	Harpacticoida	Harpacticoida
7	Kinorhyncha	Kinorhyncha
8	Mollusca	Mollusca
9	Mite	Mite
10	Nematoda	Nematoda
11	Oligochaeta	Oligochaeta
12	Ostracoda	Ostracoda
13	Tardigrada	Tardigrada
14	*	Polychaeta
15	*	Turbellaria

\*) Not found.

**Meiobenthos density.** The density analysis found that in Malayang Beach (Figure 2a), the highest density was recorded in Harpacticoida, 9,332.58 ind  $m^{-2}$  (49.92%), followed by Nematoda, 6419.66 ind  $m^{-2}$  (34.34%), then Copepoda, 480.77 ind  $m^{-2}$  (2.57%), and Cyclopoida, 339.37 ind  $m^{-2}$  (1.82%), respectively. In Tongkeina Beach (Figure 2b), the same taxa were also found with the same rank, Harpacticoida, 6476.24 ind  $m^{-2}$  (39.21%), followed by Nematoda, 6363.12 ind  $m^{-2}$  (38.53%), then Copepoda, 763.57 ind  $m^{-2}$  (4.62%), and Cyclopoida, 395.93 ind  $m^{-2}$  (2.40%), respectively.

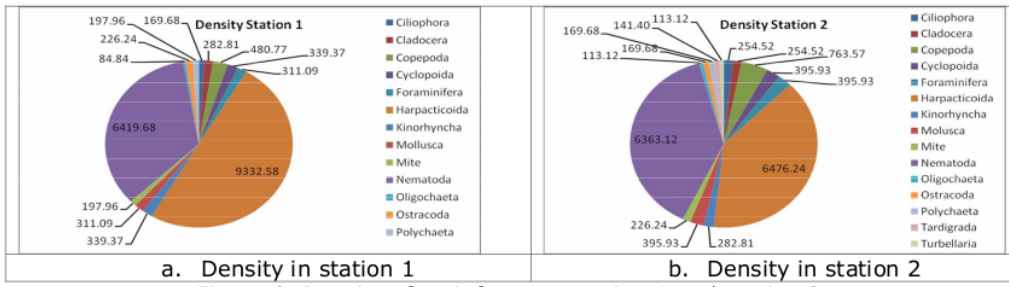


Figure 2. Density of meiofauna at station 1 and station 2.

Todaro et al (2006) recorded 16 species of meiobenthos in Mediterranean Sea cave, 1.3-2.6% of total numbers, with a density of 8.4 ind  $10 \text{ cm}^{-2}$  in November and 27.4 ind  $10 \text{ cm}^{-2}$  in June. Ansari & Parulekar (1994) who studied in seagrass meadow of Lakshadweep Atolls, Arabeen Sea, found that the abundance of meiofauna in the seagrass bed *Thalassia hemprichii* ranged between 554 and 1,351.10 ind  $\text{cm}^{-2}$ . Number of meiofauna taxa found consisted of 4 dominant groups, in which Nematoda and Copepoda cover more than 70% fauna.

**Meiobenthos diversity, dominance, and evenness.** The present study showed that the diversity in Tongkeina Beach (station 2), 1.5302, was higher than that in station 1 (Malayang Beach), 1.3702. The dominance value in station 1 (0.3690) is higher than that in station 2 (0.3073), while the evenness value in station 1 (0.5342) is lower than that in station 2 (0.5651). Based on results above, it is apparent that diversity has an inverse relationship with dominance, where when diversity is high, the dominance is low and vice versa.

The diversity value in both stations is categorized as low, which means that the diversity has a small population (Brower & Zar 1977). Although the dominance value is different, based on the criteria value (Odum 1971) due to the value is far from 1, there is nearly no dominance in either station 1 or station 2.

The evenness index in station 1 and station 2 is about 0.5 (Figure 3). Odum (1971) stated that the evenness value of a species ranges from 0 to 1. The smaller the evenness index value, the stronger the species dominance in the population. Therefore, this study indicates that the distribution of each species is the same or not much different.

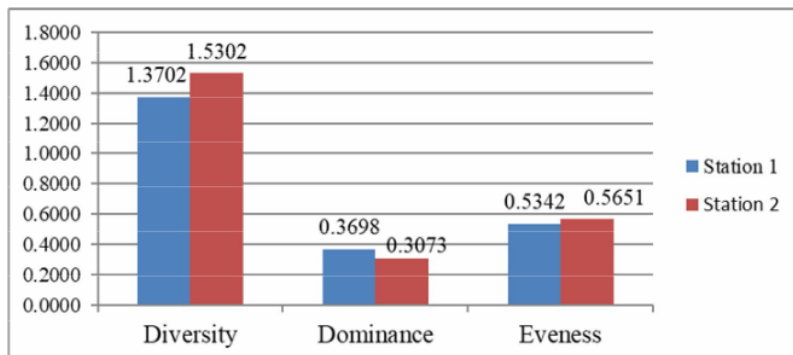


Figure 3. Diversity, dominance, and evenness indexes.

**Morphometry of meiobenthos.** Principal component analysis (PCA) with the correlation coefficient method yielded the following results (Table 3).

42  
Eigen values at station 1 and station 2

Table 3

	Station 1			Station 2		
	F1	F2	F3	F1	F2	F3
Eigenvalue	5.6299	2.1425	1.5261	5.2665	2.1701	1.4569
Variability (%)	51.1808	19.4770	13.8735	47.8777	19.7286	13.2447
Cumulative %	51.1808	70.6577	84.5312	47.8777	67.6063	80.8509

Note: F1 = the first axis; F2 = the second axis; F3 = the third axis.

Based on the value of the correlation matrix, several variables have relationships with other variables in station 1 and station 2 (Table 4 and Table 5). The relationship is weak, since the correlation matrix has a correlation coefficient value for other variables below 0.5 in station 1 (Table 4) including CI, FX and AR, and in station 2 (Table 5) it occurs only on FX. This shows that the variable with correlation coefficient below 0.5 has a great chance to become the independent variable. In the context of PCA, variables with a value below 0.5 need to be considered as well as their role in the model by looking at their position on axis 1. If they approach axis 1, the effect on the model is quite large, especially the closer to the correlation circle, but if it is far from axis 1 (in this case close to axis 2) and away from the correlation circle, the effect is quite small, so that the chances of reducing these variables in the model are quite large. The relationship is quite strong, if the correlation coefficients of other variables are above 0.5. In station 1 (Table 4), these are AA, PE, F, FY, FA, MF, RO and SO variables and in station 2 (Table 5), these cover AA, PE, CI, F, FY, FA, MF, AR, RO and SO variables.

The correlation between variables in station 1 and station 2 (Table 4 and Table 5) can be divided into 2 groups, (a) positive correlation and (b) negative correlation. Positive correlation is indicated with the positive value meaning that a variable has the same direction as the others. In other words, if a variable has increased in the model then other variables (which are correlated with it) will also increase. Negative correlation is characterized by a negative value meaning that a variable with other variables (which correlates with it) has the opposite direction, or in other words if a variable has increased in the model, the other variables (which correlate with it) will decrease.

The cumulative eigen value of station 1 shows that the variance on axes 1 (F1) to 2 (F2) reaches 0.7066 meaning that 70.66% of the data variance could explain up to the second axis, while the remaining 29.34.30% is explained by axis 3 to axis 8. If axis 3 is included to explain the data variance, the value reaches 84.53%. In station 2 (Table 3), the eigen value (characteristic root) shows that the variance on axis 1 to axis 2 reaches 0.6761, meaning that 67.61% of the data variance can explain up to the axis 2, while the remaining 32.29% is explained by axis 3 to axis 8. If axis 3 is included to explain the

data variance, the value reaches 80.85%. Thus, PCA analysis can be relied upon to analyze the meiobenthos morphometric issue above in both stations. If the cumulative value of the variance of eigen value in up to the axis 3 (F3) does not reach 80% then PCA cannot be relied on to analyze the problem above.

Table 4  
Correlation matrix (Pearson (n)) of station 1

Variables	AA	PE	CI	F	FX	FY	FA	MF	AR	RO	SO
AA	<b>1</b>	<b>0.97</b>	-0.33	<b>0.97</b>	-0.38	0.24	<b>0.76</b>	<b>0.85</b>	0.29	-0.43	-0.45
PE	<b>0.97</b>	<b>1</b>	-0.49	<b>0.98</b>	-0.34	0.34	<b>0.71</b>	<b>0.90</b>	0.33	-0.51	<b>-0.62</b>
CI	-0.33	-0.49	<b>1</b>	-0.44	-0.03	-0.20	-0.25	-0.38	-0.41	<b>0.72</b>	<b>0.70</b>
F	<b>0.97</b>	<b>0.98</b>	-0.44	<b>1</b>	-0.31	0.23	<b>0.78</b>	<b>0.81</b>	0.43	-0.55	-0.53
FX	-0.38	-0.34	-0.03	-0.31	<b>1</b>	0.16	-0.40	-0.32	0.53	-0.01	0.44
FY	0.24	0.34	-0.20	0.23	0.16	<b>1</b>	-0.09	<b>0.61</b>	-0.18	0.15	-0.50
FA	<b>0.76</b>	<b>0.71</b>	-0.25	<b>0.78</b>	-0.40	-0.09	<b>1</b>	0.50	0.30	-0.45	-0.34
MF	<b>0.85</b>	<b>0.90</b>	-0.38	<b>0.81</b>	-0.32	<b>0.61</b>	0.50	<b>1</b>	0.01	-0.24	<b>-0.66</b>
AR	0.29	0.33	-0.41	0.43	0.53	-0.18	0.30	0.01	<b>1</b>	<b>-0.69</b>	0.11
RO	-0.43	-0.51	<b>0.72</b>	-0.55	-0.01	0.15	-0.45	-0.24	<b>-0.69</b>	<b>1</b>	0.37
SO	-0.45	<b>-0.62</b>	<b>0.70</b>	-0.53	0.44	-0.50	-0.34	<b>-0.66</b>	0.11	0.37	<b>1</b>

Notes: numbers in bold indicate sufficient to large correlation; AA = area; PE = perimeter; CI = circularity; F = feret; FX = feret X; FY = feret Y; FA = feret angel; MF = min feret; AR = aspect ratio; RO = round; SO = solidity.

Table 5  
Correlation matrix (Pearson (n)) of station 2

Variables	AA	PE	CI	F	FX	FY	FA	MF	AR	RO	SO
AA	<b>1.00</b>	<b>0.99</b>	-0.30	<b>0.97</b>	-0.32	0.38	<b>0.61</b>	<b>0.89</b>	0.23	-0.36	-0.36
PE	<b>0.99</b>	<b>1.00</b>	-0.42	<b>0.98</b>	-0.28	0.41	<b>0.62</b>	<b>0.91</b>	0.28	-0.41	-0.46
CI	-0.30	-0.42	<b>1.00</b>	-0.41	-0.05	-0.11	-0.20	-0.29	-0.44	<b>0.70</b>	<b>0.68</b>
F	<b>0.97</b>	<b>0.98</b>	-0.41	<b>1.00</b>	-0.28	0.30	<b>0.70</b>	<b>0.84</b>	0.39	-0.46	-0.44
FX	-0.32	-0.28	-0.05	-0.28	<b>1.00</b>	0.20	-0.39	-0.27	0.49	0.01	0.42
FY	0.38	0.41	-0.11	0.30	0.20	<b>1.00</b>	-0.06	<b>0.62</b>	-0.19	0.14	-0.29
FA	<b>0.61</b>	<b>0.62</b>	-0.20	<b>0.70</b>	-0.39	-0.06	<b>1.00</b>	0.51	0.19	-0.20	-0.39
MF	<b>0.89</b>	<b>0.91</b>	-0.29	<b>0.84</b>	-0.27	<b>0.62</b>	0.51	<b>1.00</b>	-0.03	-0.13	-0.48
AR	0.23	0.28	-0.44	0.39	0.49	-0.19	0.19	-0.03	<b>1.00</b>	<b>-0.69</b>	0.08
RO	-0.36	-0.41	<b>0.70</b>	-0.46	0.01	0.14	-0.20	-0.13	<b>-0.69</b>	<b>1.00</b>	0.30
SO	-0.36	-0.46	<b>0.68</b>	-0.44	0.42	-0.29	-0.39	-0.48	0.08	0.30	<b>1.00</b>

Notes: numbers in bold indicate sufficient to large correlation; AA = area; PE = perimeter; CI = circularity; F = feret; FX = feret X; FY = feret Y; FA = feret angel; MF = min feret; AR = aspect ratio; RO = round; SO = solidity.

Furthermore, in the context of PCA, eight variables in station 1 (AA, PE, F, FY, FA, MF, RO and SO) (Figures 4 and 5) and ten variables in station 2 (AA, PE, CI, F, FY, FA, MF, AR, RO and SO) (Figures 4 and 5) also need to see their role in the model by looking at their position on axis 1 (F1). If it approaches axis 1, the effect on the model is quite large, especially the closer to the correlation circle, but if it is far from axis 1 (in this case, it is close to axis 2) and far from the correlation circle, the effect is quite small. On the other hand, if several variables are unidirectional and both approach axis 1, it is necessary to look at the closest one to the correlation circle. The closer the correlation circle is, the higher the chance to represent the variable that has the same direction, and conversely, the farther from the correlation circle for variables that are along one axis, the greater the chance it will be reduced from the model.

PCA analysis indicated different effect of human activities on the sea dynamic processes between station 1 and station 2. Station 1 is used as transportation lane for traditional fishing activities using small traditional boat with or without outboard engine, while station 2 is more dominantly used by bigger boats for tourist transportation to Bunaken National Park. The negative impact could be caused by fuel disposal from the boats and organic wastes as food dumped into the sea.

According to Schratzberger & Somerfield (2020), anthropogenic disturbance can facilitate new interactions among meiofauna species and between meiofauna and other benthic organisms, but the extent of the interaction is likely restricted. Wang et al (2020) added that the occurrence of meiofauna and macrofauna triggers different aspects of the microbial community that affect the litter decomposition as function of leaf quality. The present study suggested that meiofauna increased the trophic complexity and modulated their interactions with microbes.

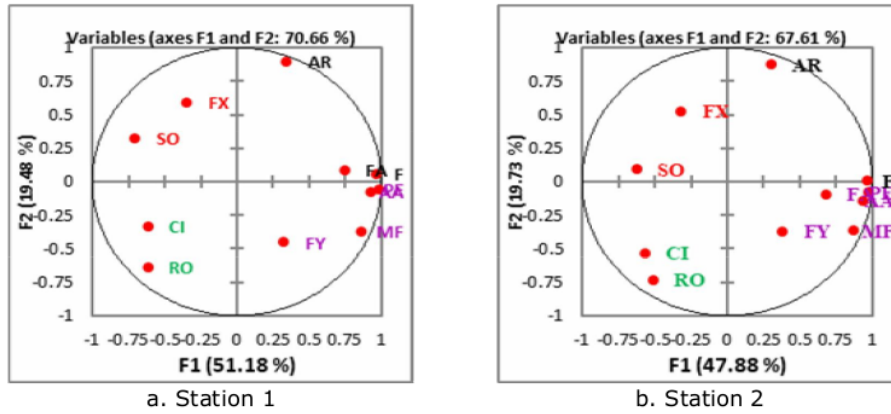


Figure 4. Circular correlation between variables on the main axis (F1 and F2).

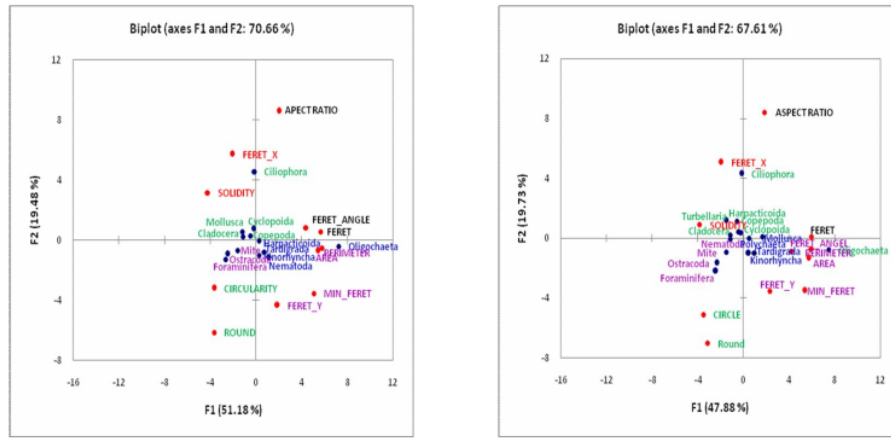


Figure 5. Distribution of taxa on the main axis biplot (F1 and F2).

The correlation between variables and the main axis can be seen in the correlation circle, in which the variable coordinate or the quality of the variables on the main axis is indicated by the distance to the F1 axis (Figures 4 and 5). The closer the variable to the axis, the greater the correlation (positive or negative) will be. The interpretation of variables that affect meiobenthos morphometry could be seen in the correlation circle of axis 1 and axis 2 (F1-F2) in station 1 (Figures 4a and 4b) and in station 2 (Figures 5a and 5b).

Figures 4a and 4b in station 1 show that the taxa have a high morphometric role (blue taxa), especially Oligochaeta that represents Harpacticoida, Tardigrada, Kinorhyncha and Nematoda because they have the same positive vector direction to morphometric size of meiobenthos FA, F, PE, AA and MF approaching to F1 axis and the circumference of the positive correlation, whereas the morphometry of FY tends to be reduced because it is closer to the F2 axis and away from the correlation circle. Ciliophora

taxa (green) represent Cyclopida, Mollusca, Cladocera and Copepoda that have the same negative vector direction to the morphometric size of meiobenthos FX and SO. For Foraminifera, Ostracoda and Mite (purple), it is sufficient to contribute values to the morphometric size of CI and RO, but CI and RO tend to be directly reduced because their role in the PCA analysis approaching to F2 axis is very small and far from the correlation circle.

Figures 5a and 5b show that in station 2, the taxa having a high morphometric role (blue taxa) are especially Oligochaeta that represents Tardigrada and Kinorhyncha because they have the same positive vector direction to the morphometric size of meiobenthos FA, PE, FA, AA and MF that are close to the F1 axis and the circumference of the positive correlation, while FY morphometry tends to be reduced because it is closer to the F2 axis and away from the correlation circle. Ciliophora (green) represents Turbellaria, Harpacticoida, Copepoda, Mollusca, Polychaeta and Nematoda which have the same negative vector direction to the morphometric measures of meiobenthos FX and SO. Foraminifera, Ostracoda, Mite and Cladocera (purple) are sufficient to contribute values to the morphometric size of CI and RO, but CI and RO tend to be directly reduced because their role in PCA analysis is very small and approaches to the F2 axis and is far from circular correlation.

**Granulometric analysis.** Sediment classification was carried out using the AFNOR classification basis. The sediment composition in station 1 consisted of 8.4% gravel, 9.86% coarse sand, 8.84% medium sand, 51.24% sand, 17.16% very fine sand, and 4.5% dust. In station 2, the sediment consisted of 0% gravel, 0.82% coarse sand, 3.47% medium sand, 36.57% sand, 50.29% very fine sand, and 8.85% dust (Figure 6).

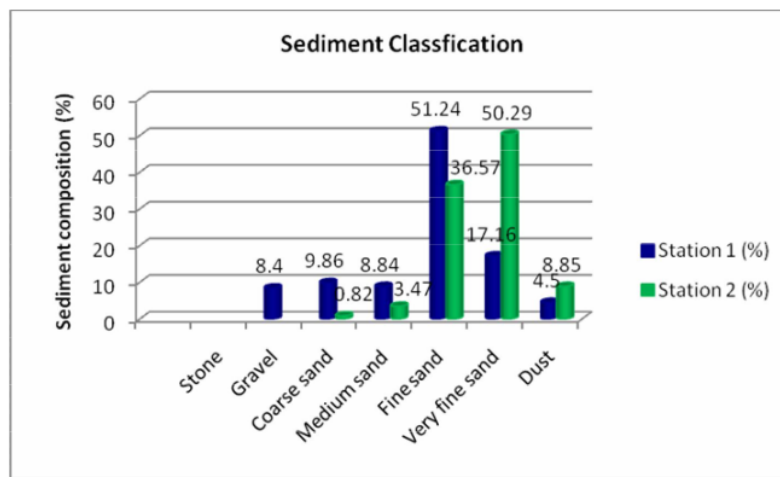
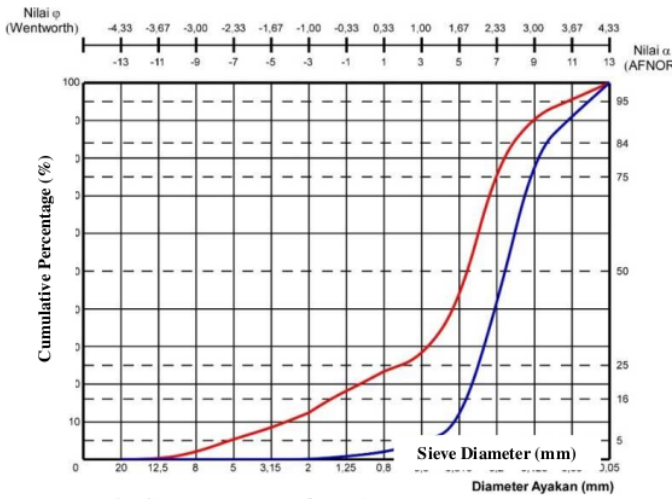


Figure 6. Sediment composition in station 1 and station 2.

The cumulative percent data are presented in Figure 7. The graph for the interpretation of the sediment granulometric distribution is made using the Canvas software. The sediment composition is also displayed in the form of a sediment composition chart. The appearance of the sediment composition in graphic form generally makes it easier to interpret the different sediment composition in different spaces.

The sediment curve for  $\phi$  (phi) interpretation can be perfectly drawn using the Canvas software (Figure 7), since Canvas software provides drawing facilities through the data coordinate filling technique so that the data input process could be precisely done.



Notes:

— Sediment curve of station 1  
— Sediment curve of station 2

Figure 7. Sediment curve for interpretation of variables in sediment granulometry distribution.

Interpolation of various  $\varphi$  values for sediment granulometric distribution analysis can be carried out after the curve has been formed. The trick is to precisely place the cursor position at the intersection of the curve line and the horizontal line of the  $\varphi$  value you are estimating. The data in the form of the cursor position in the Canvas software become input data for the calculation process using Microsoft Excel data processing software. The values of  $\varphi$  and the sediment granulometric distribution variables are presented in Table 6.

Table 6  
Variable interpolation for  $\varphi$  value

Sampling equipment	Sampling location	Sediment granulometric distribution variables						
		$\varphi_5$	$\varphi_{16}$	$\varphi_{25}$	$\varphi_{50}$	$\varphi_{75}$	$\varphi_{84}$	$\varphi_{95}$
Corer spuit	Station 1	-2.856	-0.893	0.409	1.704	1.806	2.388	3.134
Corer spuit	Station 2	1.050	1.719	1.765	2.367	2.465	3.030	3.729

Granulometric analysis of sediment distribution is a description regarding the concentration and distribution of the grain size of the studied sediments. The empirical mean describes the concentration of the sediment grain size. Sorting provides an overview regarding the sorting of sediment grain sizes. The worse the criteria, the more diverse the sediment size. The slope provides an illustration of the curvature of the sediment graph curve, in which symmetrical granulometry indicates that the curve is close to normal. Tapering is a depiction of the smoothness of the formed sediment curve, in which the closer to the leptokurtic shape, the curve is getting tapered (Table 7).

Table 7  
Sediment granulometric distribution variables

Sampling equipment	Sampling location	Sediment granulometric distribution variables							
		Mz	Cr	$\sigma_1$	Cr	Sk <sub>i</sub>	Cr	KG	Cr
Corer spuit	Station 1	-0.070	Cm	1.73	Bs	-0.55	Sals	1.76	SL
Corer spuit	Station 2	0.794	RS	0.73	Um	0.01	SG	1.57	SL

Notes: Mz = empirical mean; Cr = criteria;  $\sigma_1$  = sorting; Sk<sub>i</sub> = skewness; KG = curtosis; Cm = clay/mud; Bs = badly sorted, Sals = strong asymmetry to large sizes, SL = very leptokurtic, RS = rough sands; Um = unsorted medium; SG = symmetric granulometry.

**Conclusions.** There were 13 taxa found in station 1 (Malalayang Beach), Ciliophora, Cladocera, Copepoda, Cyclopoida, Foraminifera, Harpacticoida, Kinorhyncha, Mollusca, Mite, Nematoda, Oligochaeta, Ostracoda and Tardigrada and 15 taxa in station 2 (Tongkeina Beach), Ciliophora, Cladocera, Copepoda, Cyclopoida, Foraminifera, Harpacticoida, Kinorhyncha, Molluscs, Mite, Nematoda, Oligochaeta, Ostracoda and Tardigrada plus two more taxa Polychaeta and Turbellaria.

The highest density of meiobenthos taxa in Manado Beach was record<sup>21</sup> in Harpacticoida, followed by Nematoda, then Copepod<sup>39</sup> and Cyclopoida. Diversity index was higher in stati<sup>21</sup> 2 than station 1, the dominance was higher station 1 than station 2, and the evenness index was higher in station 2 than station 1.

In station 1, the taxa which have a high morphometric role, especially Oligochaeta, have the role of representing Harpacticoida, Tardigrada, Kinorhyncha and Nematoda taxa because they have the same positive vector direction to the morphometric measurements of meiobenthos FA, F, PE AA and MF that approach the F1 axis and the positive correlation circumference, whereas FY morphometry tends to be reduced because it is closer to the F2 axis and away from the correlation circle. For Ciliophora represents Cyclopoida, Mollusca, Cladocera and Copepoda which have the same negative vector direction to the meiobenthos FX and SO morphometric sizes. Foraminifera, Ostracoda and Mite have a significant role in contributing values to the morphometric size of CI and RO, but whereas RO tends to be directly reduced because their role in the model in the PCA analysis is very small and far from the correlation circle. Sediment classification was carried out using the AFNOR classification basis.

The sediment composition (%) in station 1 consisted of 8.4% gravel, 9.86% coarse sands, 8.84% medium sand, 51.24% sand, 17.16% very fine sand, and 4.5% dust. The sediment in station 2 consisted of 0% gravel, 0.82% coarse sands, 3.47 % medium sand, 36.57% sand, 50.29% very fine sand, and 8.85% dust.

## References

- Ansari Z., Parulekar A. H., 1994 Meiobenthos in the sediments of seagrass meadows of Lakshadweep Atolls, Arabian Sea. *Vie et Milieu* 44(3-4):185-190.
- Brower J. E., Zar J. H., 1977 Field and laboratory method for general ecology. William C. Brown Company, Dubuque, Iowa, 273 pp.
- Coull B. C., 1988 Ecology of the marine meiofauna. In: Introduction to the study of meiofauna. Hinggins R. P., Thiel H. (eds), Smithsonian Institution Press: Washington D.C., pp. 18-38.
- Coull B. C., Chandler G. T., 2001 Meiobenthos. In: Encyclopedia of ocean sciences. Steele J. H., Turekian K., Thorpe S. A. (eds), Academic Press, London, pp. 1705-1711.
- Dyer K. D., 1986 Coastal and estuarine sediment dynamics. John Wiley and Sons, Chichester, 358 pp.
- Eleftheriou A., 2013 Methods for the study of marine benthos. Fourth edition, Wiley-Blackwell, 496 pp.
- Giere O., 2009 Meiobenthology. The microscopic motile fauna of aquatic sediments. Second edition, Springer-Verlag Berlin Heidelberg, 527 pp.
- Higgins R. P., Thiel H., 1988 Introduction to the study of meiofauna. Smithsonian Institution Press: Washington D.C., 488 pp.
- Krebs C. J., 1989 Ecological methodology. Harper & Row, New York, 654 pp.
- Lee M., 2018 Extraction of meiofauna using simple decantataion. Available at: [http://meiochile.matthewlee.org/?page\\_id=171](http://meiochile.matthewlee.org/?page_id=171). Accessed: August, 2019. <sup>26</sup>
- Legendre P., Legendre L., 2012 Numerical ecology. Third edition. Elsevier, 1006 pp.
- Odum E. P., 1971 Fundamentals of ecology. Third Edition, W.B. Saunders Co., Philadelphia, 574 pp.
- Schratzberger M., Somerfield P. J., 2020 Effects of widespread human disturbances in the marine environment suggest a new agenda for meiofauna research is needed. *Science of the Total Environment* 728:138435.

11

Somerfield P. J., Warwick R. M., 2013 Meiofauna techniques. In: Methods for the study of marine benthos. 4th edition. Eleftheriou A. (ed), John Wiley & Sons, Ltd., Chichester, UK, pp. 253-284.

Todaro M. A., Leasi F., Bizzarri N., Tongiorgi P., 2006 Meiofauna densities and gastrotrich community composition in a Mediterranean Sea cave. *Marine Biology* 149:1079-1091.

9

Wang F., Lin D., Li W., Dou P., Han L., Huang M., Qian S., Yao J., 2020 Meiofauna promotes litter decomposition in stream ecosystems depending on leaf species. *Ecology and Evolution* 10(17):9257-9270.

35

Received: 11 February 2021. Accepted: 08 March 2021. Published online: 01 April 2021.

Authors: 3

Agung B. Windarto, Faculty of Fisheries and Marine Science, Sam Ratulangi University, Jln. Kampus-Bahu, Manado-95115, Indonesia, e-mail: agungwindarto115@unsrat.ac.id

Royke M. Rampengan, Faculty of Fisheries and Marine Science, Sam Ratulangi University, Jln. Kampus-Bahu, Manado-95113, Indonesia, e-mail: roy\_rampengan@yahoo.com

Esry T. Opa, Faculty of Fisheries and Marine Science, Sam Ratulangi University, Jln. Kampus-Bahu, Manado-95115, Indonesia, e-mail: esrytommyop@yahoo.com

Silvester B. Pratasik, Faculty of Fisheries and Marine Science, Sam Ratulangi University, Jln. Kampus-Bahu, Manado-95115, Indonesia, e-mail: spjong07@yahoo.com

This is an open-access article distributed under the terms of the Creative Commons Attribution License, which permits unrestricted use, distribution and reproduction in any medium, provided the original author and source are credited.

How to cite this article:

Windarto A. B., Rampengan R. M., Opa E. T., Pratasik S. B., 2021 Study of meiobenthos community in Manado Beach, North Sulawesi. AACL Bioflux 14(2):884-896.

17

AACL Bioflux, 2021, Volume 14, Issue 2.  
<http://www.bioflux.com.ro/aacl>

# Study of meiobenthos community in Manado Beach, North Sulawesi

ORIGINALITY REPORT



PRIMARY SOURCES

- |   |   |    |
|---|---|----|
| 1 | <a href="http://mafiadoc.com">mafiadoc.com</a><br>Internet Source   | 2% |
| 2 | <a href="http://www.bioflux.com.ro">www.bioflux.com.ro</a><br>Internet Source   | 1% |
| 3 | Oda, Taiko, Jong-Soo Lee, Yuta Sato, Yasuaki Kabe, Satoshi Sakamoto, Hiroshi Handa, Remy E. P. Mangindaan, and Michio Namikoshi.<br>"Inhibitory Effect of N,N-Didesmethylgrossularine-1 on Inflammatory Cytokine Production in Lipopolysaccharide-Stimulated RAW 264.7 Cells", Marine Drugs, 2009.<br>Publication | 1% |
| 4 | <a href="http://www.preprints.org">www.preprints.org</a><br>Internet Source   | 1% |
| 5 | <a href="http://people.uea.ac.uk">people.uea.ac.uk</a><br>Internet Source   | 1% |
| 6 | <a href="http://spectrum.troy.edu">spectrum.troy.edu</a><br>Internet Source   | 1% |

- 7 Andrew S. Green, G. Thomas Chandler. "Meiofaunal bioturbation effects on the partitioning of sediment-associated cadmium", Journal of Experimental Marine Biology and Ecology, 1994  
Publication
- 
- 8 paduaresearch.cab.unipd.it 1 %  
Internet Source
- 
- 9 Ignacio Peralta-Maraver, Rachel Stubbington, Shai Arnon, Pavel Kratina et al. "The riverine bioreactor: An integrative perspective on biological decomposition of organic matter across riverine habitats", Science of The Total Environment, 2021  
Publication
- 
- 10 explora.unex.es <1 %  
Internet Source
- 
- 11 researchrepository.murdoch.edu.au <1 %  
Internet Source
- 
- 12 imagej.nih.gov <1 %  
Internet Source
- 
- 13 journals.plos.org <1 %  
Internet Source
- 
- 14 Jonathan Ruiz-Jaramillo, Laura Montiel-Vega, Luis José García-Pulido, Carmen Muñoz-González, Álvaro Blanca-Hoyos. "Ambient <1 %

Vibration as a Basis for Determining the Structural Behaviour of Watchtowers against Horizontal Loads in Southeast Spain", Applied Sciences, 2020

Publication

---

- |    |   |      |
|----|---|------|
| 15 | <a href="http://zookeys.pensoft.net">zookeys.pensoft.net</a>  | <1 % |
| 16 | "Meiobenthology", Springer Science and Business Media LLC, 2009   | <1 % |
| 17 | <a href="http://www.readkong.com">www.readkong.com</a>  | <1 % |
| 18 | <a href="http://digital.library.unt.edu">digital.library.unt.edu</a>  | <1 % |
| 19 | <a href="http://zoologicalstudies.springeropen.com">zoologicalstudies.springeropen.com</a>  | <1 % |
| 20 | <a href="http://eprints.soton.ac.uk">eprints.soton.ac.uk</a>  | <1 % |
| 21 | Francesca Cima, Loriano Ballarin. "A proposed integrated bioindex for the macrofouling biocoenosis of hard substrata in the lagoon of Venice", Estuarine, Coastal and Shelf Science, 2013 | <1 % |
| 22 | <a href="http://www.gastrotricha.unimore.it">www.gastrotricha.unimore.it</a>  | <1 % |

- 23 [www.mdpi.com](http://www.mdpi.com) Internet Source <1 %
- 24 I Dewiyanti, M Harbi, S A ElRahimi, M Ulfah, A Damora. "Community structure of gastropods and bivalves associated in mangrove ecosystem at Pusung Cium Island, Seruway, Aceh Tamiang", IOP Conference Series: Earth and Environmental Science, 2021 Publication <1 %
- 25 Nineteenth International Seaweed Symposium, 2009. Publication <1 %
- 26 [ejournal-balitbang.kkp.go.id](http://ejournal-balitbang.kkp.go.id) Internet Source <1 %
- 27 [upcommons.upc.edu](http://upcommons.upc.edu) Internet Source <1 %
- 28 Westaway, K.E.. "Reconstructing the geomorphic history of Liang Bua, Flores, Indonesia: a stratigraphic interpretation of the occupational environment", Journal of Human Evolution, 200911 Publication <1 %
- 29 Gheskiere, T.. "Nematodes from wave-dominated sandy beaches: diversity, zonation patterns and testing of the isocommunities concept", Estuarine, Coastal and Shelf Science, 200501 <1 %

- 30 R Ambo-Rappe, C Rani. "Physical structure of artificial seagrass affects macrozoobenthic community recruitment", Journal of Physics: Conference Series, 2018 <1 %
- Publication
- 
- 31 [www.redalyc.org](http://www.redalyc.org) <1 %
- Internet Source
- 
- 32 [www.vliz.be](http://www.vliz.be) <1 %
- Internet Source
- 
- 33 L. Levin, D. Gutiérrez, A. Rathburn, C. Neira, J. Sellanes, P. Muñoz, V. Gallardo, M. Salamanca. "Benthic processes on the Peru margin: a transect across the oxygen minimum zone during the 1997–98 El Niño", Progress in Oceanography, 2002 <1 %
- Publication
- 
- 34 [palaeo-electronica.org](http://palaeo-electronica.org) <1 %
- Internet Source
- 
- 35 [hrmars.com](http://hrmars.com) <1 %
- Internet Source
- 
- 36 C Octavina, N M Razi, M Agustiar, R Sakinah, M R Fazillah, A Sahidin. "Biological community structure in Krueng Sarah River, Aceh Besar District", IOP Conference Series: Earth and Environmental Science, 2021 <1 %
- Publication
-

- 37 Fengchao Li, Yumimg Mei. "Use of Microbial Community Characteristics in Assessment of Water Quality in Baiyangdian Lake", 2010 4th International Conference on Bioinformatics and Biomedical Engineering, 2010 <1 %  
Publication
- 
- 38 Mark M. Goldman. "Transient electromagnetic inversion based on an approximate solution to the forward problem", GEOPHYSICS, 1988 <1 %  
Publication
- 
- 39 Mengxu Zhao, Bo-Ping Han. "Chapter 8 A Peridinium Bloom in a Large Narrow Impoundment, Huanglongdai Reservoir, Southern China", Springer Nature, 2012 <1 %  
Publication
- 
- 40 V. C. Sarmento, P. J. P. Santos. "Trampling on coral reefs: tourism effects on harpacticoid copepods", Coral Reefs, 2011 <1 %  
Publication
- 
- 41 Yong Xu, Jixing Sui, Xinzhen Li, Hongfa Wang, Baolin Zhang. "Variations in macrobenthic community at two stations in the southern Yellow Sea and relation to climate variability (2000–2013)", Aquatic Ecosystem Health & Management, 2018 <1 %  
Publication
- 
- 42 link.springer.com <1 %  
Internet Source

43

idoc.pub  
Internet Source

<1 %

44

Isibor Omoregie, Igbinovia Osahenrunmwen,  
Aworunse Samuel, Taiwo Samson, Ige Joseph.  
"Application of Antioxidant Enzymes as  
Biomarkers in Cultivability Assessment of  
Palaemonid Shrimps", Annual Research &  
Review in Biology, 2017

<1 %

Publication

Exclude quotes Off

Exclude matches Off

Exclude bibliography Off